Immunoediting of Cancers May Lead to Epithelial to Mesenchymal Transition[1]

Keith L. Knutson,[2]* Hailing Lu,† Brad Stone,‡ Jennifer M. Reiman,* Marshall D. Behrens,* Christine M. Prosperi,* Ekram A. Gad,† Arianna Smorlesi,[3]† and Mary L. Disis†

Tumors evade both natural and pharmacologically induced (e.g., vaccines) immunity by a variety of mechanisms, including induction of tolerance and immunoediting. Immunoediting results in reshaping the immunogenicity of the tumor, which can be accompanied by loss of Ag expression and MHC molecules. In this study, we evaluated immunoediting in the neu-transgenic mouse model of breast cancer. A tumor cell line that retained expression of rat neu was generated from a spontaneous tumor of the neu-transgenic mouse and, when injected into the non-transgenic parental FVB/N mouse, resulted in the development of a strong immune response, initial rejection, and ultimately the emergence of neu Ag-loss variants. Morphologic and microarray data revealed that the immunoedited tumor cells underwent epithelial to mesenchymal transition accompanied by an up-regulation of invasion factors and increased invasiveness characteristic of mesenchymal tumor cells. These results suggest that immunoediting of tumor results in cellular reprogramming may be accompanied by alterations in tumor characteristics including increased invasive potential. Understanding the mechanisms by which tumors are immunoedited will likely lead to a better understanding of how tumors evade immune detection. *The Journal of Immunology,* **2006, 177: 1526–1533.**

A key function of the immune system is to survey for dysfunctional tissues such as cancers. Research indicates that tumors evade the immune system following immunosurveillance by either directly inducing tolerance or by altering their phenotype to suppress or evade immunity. This latter mechanism has been termed immunoediting (1). The occurrence of immunoediting is becoming more frequent as our ability to modulate antitumor immunity improves. Some important examples of immunoediting are modulation of Ag expression (Ag-loss variants) and loss of immune recognition molecules. The ability of a tumor cell to modulate or reduce levels of expression of Ags has been increasingly reported using a variety of different immunotherapy approaches to demonstrate that immunoediting can be induced pharmacologically (2–7). Natural immunoediting is supported by studies that have demonstrated that as tumors age, the expression of important recognition molecules decrease. For example, studies in breast cancer have revealed that most advanced tumors have little or no expression of MHC class I molecules unlike normal breast epithelium or early cancers, which typically express an abundance of the molecule (8).

The mechanisms by which immunoediting occurs remain largely unknown. The loss of Ags could simply reflect changes such as gene mutagenesis, which leads to loss of specific gene expression. Alternatively, the immune system could lead to the activation of pathways that lead to rapid, sustained changes in broad gene expression profiles in tumor cells (i.e., cellular reprogramming). This ability of tumors to adapt to a new microenvironment by reprogramming reflects an important property of tumors called plasticity (9).

We, and others, have found that tumors arising in the FVB/N rat neu-transgenic (neu-tg)[4] mouse are capable of rapid immune escape when treated with any of a variety of immune-based approaches including mAb therapy, vaccines, or T cell therapy (2, 10). Furthermore, this immunoescape phenomenon can also be observed when transplanting tumors into the syngeneic non-transgenic parental FVB/N mouse (11). Immune escape observed when transplanting tumors from the neu-tg mouse into the FVB/N parental animals is manifest as the loss of neu Ag expression (2). In this study, we evaluated the phenotypic differences (i.e., immunoediting) between native neu-expressing tumor cells, derived from the neu-tg mouse, and those that resulted from immunoediting following transplantation in the FVB/N parental strain. Our results suggest that immunoedited tumors have undergone reprogramming through epithelial to mesenchymal transition (EMT).

Materials and Methods

Animals

Mice were from an established colony of neu-tg mice (strain FVB/N-TgN (MMTVneu)202Mul) or FVB/N mice (12). The neu-tg mice develop spontaneous tumors after a long latency (e.g., >50 wk), and in the current studies, our previously described transplantable model was used in mice between the ages of 6 and 12 wk (2). As previously described by others and us, the neu-tg mice are tolerant of the neu transgene. This tolerance can be circumvented with vaccines and other immune manipulations (10, 13–17). Animal care and use was in accordance with the institutional guidelines at both the Mayo Clinic (Rochester, MN) and the University of Washington (Seattle, WA).

*Department of Immunology, Mayo Clinic, Rochester, MN 55905; †Tumor Vaccine Group, Center for Translational Medicine in Women's Health, Seattle, WA 98195; and ‡Benaroya Research Institute, Seattle, WA 98101

Received for publication January 17, 2006. Accepted for publication May 16, 2006.

The costs of publication of this article were defrayed in part by the payment of page charges. This article must therefore be hereby marked *advertisement* in accordance with 18 U.S.C. Section 1734 solely to indicate this fact.

[1] This study was supported by Grants R01 CA-113861 (to K.L.K.) and R01 CA-85374 (to M.L.D.) from the National Institutes of Health. K.L.K. is supported by a National Cancer Institute Howard Temin Award K01-CA100764. M.L.D. is supported by a National Cancer Institute Career Award K24-CA85218.

[2] Address correspondence and reprint requests to Dr. Keith L. Knutson, Mayo Clinic College of Medicine, 342C Guggenheim, Mayo Clinic, 200 First Street Southwest, Rochester, MN 55905. E-mail address: knutson.keith@mayo.edu

[3] Current address: Dipartimento Ricerche, Istituto Nazionale Riposo e Cura Anziani, via Birarelli 8, 60100 Ancona, Italy.

[4] Abbreviations used in this paper: neu-tg, neu-transgenic; EMT, epithelial to mesenchymal transition; MMP, matrix metalloproteinase; TJP, tight junction protein; SI, stimulation index; MMC, mouse mammary carcinoma; ANV, Ag-negative variant.

0022-1767/06/$02.00

Cell lines

The mouse mammary carcinoma (MMC) cell line was established from a spontaneous tumor harvested from the neu-tg mice. MMC cells were grown and maintained in RPMI 1640 supplemented with 20% FCS (Gemini Bio-Products) as well as penicillin/streptomycin and L-glutamine (Invitrogen Life Technologies). Ag-negative variants (ANV) are cell lines derived from neu-loss variant tumors in FVB/N mice and are maintained in culture identical with MMC. The cell lines were not used continuously, but rather replaced with low-passage cultures every 2 mo. The microarrays were performed with different cultures to avoid intraculture artifact and biasing. Both cell lines have been previously used in other studies in the same mouse model (2, 11).

Tumor growth in vivo

The tumor cells were harvested from culture plates using 2 mM EDTA and washed before injection. FVB/N or neu-tg mice were inoculated with MMC or ANV1 cells s.c. on the right mid-dorsum with a 23-gauge needle. Tumors were measured every other day with vernier calipers, and tumor size was calculated as the product of length times width. In some cases, mice were pretreated with mAbs to deplete either $CD8^+$ or $CD4^+$ T cells before tumor injection. In these cases, mice were i.v. administered 100 μg of purified monoclonal GK1.5 (anti-CD4; American Type Collection Culture (ATCC)) or 53.6.72 (anti-CD8; ATCC) for 5 consecutive days. Mice were allowed to rest 48 h before tumor injection. Peripheral blood was analyzed for $CD4^+$ and $CD8^+$ T cells on day 5 to verify depletion as described below.

Flow cytometry

Cultured cell line cells, tumor-harvested tumor cells, and T cells were stained in PBS containing 1% FCS before labeling. Cells ($0.5–1.0 \times 10^6$) were incubated in primary anti-rat neu Ab (mAb 7.16.4, a mouse IgG2a Ab reactive with the rat neu oncogene-encoded p185 molecule was generously provided by Dr. M. Greene and has been previously described (18)), anti-CD24 FITC (BD Pharmingen), anti-MHC class I FITC (TIB-139, ATCC), anti-CD4 FITC (GK1.5), and anti-CD8 FITC (53.6.72) at 4°C for 30 min and washed three times, and in some cases, followed by secondary labeling with FITC-conjugated rat anti-mouse Ab (BD Pharmingen) at 4°C for 30 min followed by three washes. Samples were run on a FACScan II and analyzed using CellQuest software (BD Biosciences). Control cells received nonspecific mouse IgG. The relative mean fluorescence intensity was calculated as the ratio of the geometric mean of the fluorescence intensities of rat neu stained to the control IgG-stained control cells.

Proliferation assays

Proliferation assays were done essentially as previously described with minor modifications (19). Splenocytes (3–12 replicates) were plated at 5×10^5 splenocytes per well and treated with media alone, 2 μg of Con A, 1:1 irradiated (3300 rad) Con A-elicited blasts (16 h at 5 μg/ml Con A), or freeze-thaw tumor lysates (three freezes). [^{3}H]Thymidine (1.5 μCi/well) was added at 24 h following antigenic stimulation and the incorporation into the DNA was measured at 48 h by liquid scintillation. The stimulation indices (SI) were calculated as the ratio of the sample cpm to the control cpm.

Microarray analysis

RNA was extracted using an RNeasy kit (Qiagen) or RNA4 aqueous kit from Ambion. Biotinylated cRNA probes were synthesized using a MessageAmp II kit from Ambion. Two different types of microarray were used, Affymetrix and dual-label expression arrays. For the Affymetrix analysis, 15 μg of each labeled probe was mixed with Affymetrix hybridization spike controls in a standard hybridization solution and heated to 95°C for 5 min, 45°C for 5 min, centrifuged to pellet particulates, and hybridized to Affymetrix Mouse430_2 chips. Chips were washed using the supplied eukGE-WS5v2 protocol and stained using Ab amplification on a GeneChip 450 Fluidics station. Chips were immediately scanned using a GeneChip 3000 scanner. Affymetrix global scaling was used to normalize results from each sample.

For the dual-label arrays, RNA was labeled with Cy3-dUTP and Cy5-dUTP (Amersham Biosciences) by reverse transcription. For each reverse transcription reaction, 30 μg of total RNA was mixed with random hexamer in a total volume of 18.5 μl, heated at 70°C for 10 min, and placed on ice for 10 min. Unlabeled nucleotide pool with either Cy3- or Cy5-conjugated dUTP, 5× first-strand Superscript II buffer, 0.1 M DTT, Superscript II reverse transcriptase (Invitrogen Life Technologies) were added to a final volume of 30 μl. After incubation at 42°C for 2 h, RNA was hydrolyzed by adding 10 μl of 0.5 M EDTA and 10 μl of 1 N NaOH and incubated at 65°C for 15 min. The mixture was neutralized by adding 25 μl of 1 M Tris-HCl (pH 7.4) and by adjusting the volume to 500 μl with Tris-EDTA. Labeled cDNA was purified by centrifugation in a Microcon-30 concentrator (Amicon; Millipore) and eluted in water. The Cy3- and Cy5-labeled cDNAs were then quenched with hydroxylamine to prevent cross-coupling. Qiaquick PCR purification kit (Qiagen) was used to remove unincorporated/quenched dye. Hybridization and washing of the slides were done using standard protocol. Then the arrays were dried by centrifugation. Fluorescence intensities for both dyes (Cy3 and Cy5) and local background subtracted values for individual spots were obtained using the GenePix 4000 microarray scanner and accompanying software (Axon Instruments). The data were imported into Microsoft Excel spreadsheets for analysis. Defective spots that are substandard on the scanned image or have negative background subtracted values were first excluded. Then the Cy3:Cy5 ratio values were log transformed, and global equalization to remove a deviation of the signal intensity between whole Cy3 and whole Cy5 fluorescences was performed by subtracting a median of all log(Cy3/Cy5) values from each log(Cy3/Cy5) value.

Migration assay

NeuroProbe 96-well plates (5-μm pore size) were coated with 10 μg/ml fibronectin (Sigma-Aldrich) at 37°C for 1 h. Next followed removing the excess fibronectin with HBSS. Tumor cells were suspended in HBSS with 0.1% BSA at a concentration of 10^6/ml. Calcein-AM (Molecular Probes) was added to cells at a final concentration of 2 μM and incubated for 30 min at 37°C in free calcein-AM-incubated cells in RPMI 1640 and resuspended at 10^6 in RPMI 1640 and 1% DMSO. Fifty thousand cells were added to the upper chamber of the NeuroProbe plate and incubated for 90 min at 37°C. The cells that moved through the fibronectin were then quantified on a PerkinElmer Victor V using 485 nm excitation/535 nm emission program. A standard curve was generated by measuring the fluorescent intensity of varying concentrations of calcein-AM-stained cells.

RT-PCR analysis

E-cadherin, tight junction protein 1 (TJP1), vimentin transcript, and rat neu were detected in MMC and ANV cells by RT-PCR on a Bio-Rad MyCycler. Total RNA was extracted from MMC and ANV cells as already described. cDNA was synthesized from 100 ng of total RNA by SuperScript One-Step RT-PCR with Platinum Taq as per manufacturer's instructions (Invitrogen Life Technologies). RT-PCR was performed using the following primers: E-cadherin forward GGTCTTTGAGGGATTCGTTGC and reverse CAGCCTGAACCACCAGA-GTGTATG, which yielded a 248-bp product; TJP-1 forward GACTTTTGTCCCACTTGAATCCC and reverse CCACCGTCCGC ATAAACATCTC; vimentin forward TAGCCGCAGC CTCTATTCCTCATC and reverse AGAAGTCCACCGAGTCTT-GA AGC; and rat HER2/neu forward TGAGCACCATGGAGCTGGC and reverse TCCGGCAGAAATGCCAGGCTC that yielded a 1144-bp product. The PCR conditions for all primer pairs, except neu, were cDNA synthesis and predenaturation: 1 cycle at 50°C, 30 min, 94°C, 2 min; PCR amplification: 40 cycles at 94°C, 15 s (denaturation), 57.5°C, 30 s (annealing), 70°C, 15 s (extension); and final extension: 1 cycle at 72°C, 10 min. For rat neu, the PCR conditions were cDNA synthesis and predenaturation: 1 cycle at 50°C for 30 min, 94°C for 2 min; PCR amplification: 40 cycles at 94°C for 30 s (denaturation), 55.8°C for 45 s (annealing), 70°C for 3 min (extension); and final extension: 1 cycle at 72°C for 10 min. These samples were electrophoresed on a 1% agarose gel with ethidium bromide and imaged on a Gel Doc XR (Bio-Rad). The results for E-cadherin were analyzed with Quantity One software (v.4.5.2; Bio-Rad).

Western blotting

Probing for rat neu expression in tumors and tumor cell lines was performed as previously described (2).

Results

The MMC cell line is immunogenic in parental FVB/N mice and elicits a protective T cell response

The ability of the neu^+ MMC to generate tumors was examined in the neu-tg and parental rat neu^- FVB/N mice. As shown in Fig. 1*A*, tumors that were initially rejected in FVB/N parental mice emerged after a longer latency compared with the neu-tg mouse. As previously reported, implantation of the MMC tumor cells in the FVB/N is accompanied by a strong immune response, which was confirmed in this study (Fig. 1*B*) (11). Splenocytes derived

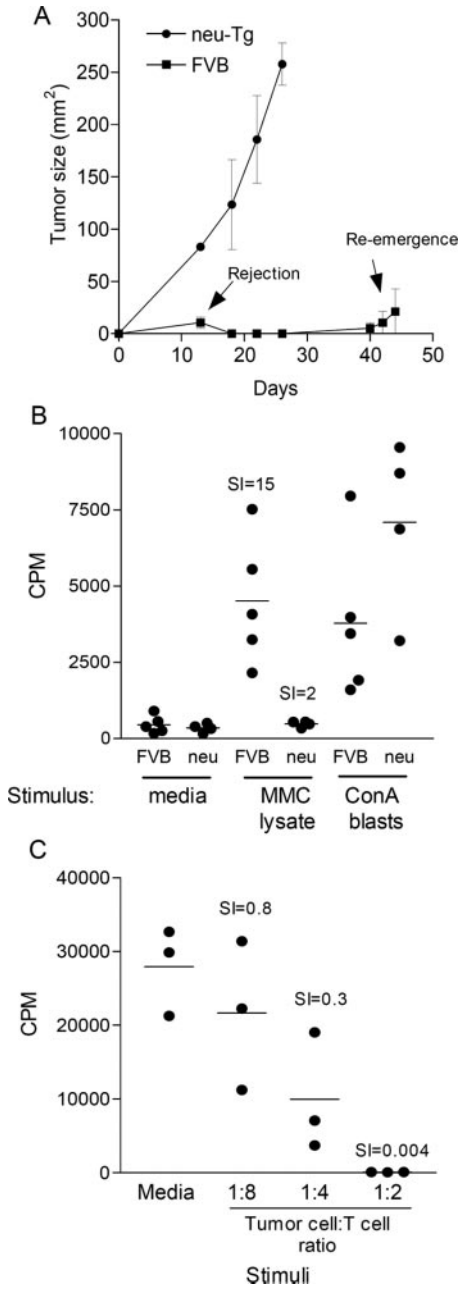

FIGURE 1. The MMC cell line is immunogenic in parental FVB/N mice and elicits a protective T cell response. *A*, Initial rejection of the MMC cells (6×10^6) in the FVB/N parental mice but not the neu-tg mice. Each time point is the mean (± SEM) of six independent measurements. Similar results were also observed in other experiments. *B*, FVB/N but not neu-tg mice demonstrate an immune response to irradiated tumor cells as assessed by proliferation assays (in cpm). Animals received an injection of live 5×10^6 MMC tumor cells and immunity was examined 1 wk later and before tumor development. The proliferation responses to irradiated Con A-elicited splenic blasts are shown as a positive control. Each data symbol represents the mean of 12 replicates from an individual mouse and is representative of two independent experiments. The solid line within each group represents the mean. Tumor cell lysates were added at a tumor cell-to-T cell ratio of 1:4. *C*, MMC-immunized FVB/N mice do not respond to tumors that emerge following rejection. Each scattergram symbol (●) represents the mean basal proliferation response (in cpm) of splenocytes incubated with either medium alone or varying concentrations of tumor cell lysates. Each dot is calculated from three dots and represents a unique mouse. The horizontal line represents the mean of the groups of three mice. The splenocytes were analyzed 2 wk after MMC tumor challenge but before the development of measurable tumors. SI values are shown in *B* and *C*.

from FVB/N mice injected with tumor demonstrated a proliferation response (SI = 15 ± 5, $n = 5$) to tumor in vitro that was significantly ($p = 0.026$) greater than the proliferation response observed by the splenocyte derived from tumor-bearing neu-tg mice (SI = 2 ± 0.5, $n = 4$). To determine whether FVB/N mice that had rejected MMC tumor challenge developed an immune response to the relapse tumors, splenocytes were assessed for reactivity, following MMC tumor rejection, to lysates derived from the relapse tumors (Fig. 1*C*). As shown, MMC-immunized mice do not demonstrate an immune proliferation response but rather are inhibited. The addition of relapse tumor lysate to splenocytes, at a 1:2 tumor cell-to-splenocyte ratio, led to a decline in baseline proliferation (SI = 0.004 ± 0.0006, $n = 3$, $p < 0.001$). This decrease was specific for the relapse tumor cells as it was observed that the addition of Con A to splenocytes from the same mice resulted in enhanced proliferation (data not shown). Although the precise mechanism by which blockade of proliferation occurs is unclear, it is possible that tumors produce immune suppressive molecules (e.g., IL-10) that dampen the splenocytes baseline growth response to serum-derived immune stimulatory molecules, which would be consistent with previous findings that Ag-loss variants that arise in these mice produce reduced "danger signals" (11). Nonetheless, what is apparent is that unlike MMC lysates (Fig. 1*B*), which stimulate proliferation, the relapsing tumors do not.

Tumors that emerge in FVB/N parental mice following MMC rejection are Ag-low variants or ANVs

The phenotype (i.e., neu expression) of the tumors derived from the neu-tg and the FVB/N mice was compared by flow cytometric analysis. Fig. 2*A* shows neu expression in the MMC cell line that was used for tumor transplant. As shown in Fig. 2, *B* and *C*, and *E* and *F*, tumors that emerged in the FVB/N mice (Fig. 2, *D–F*) had significantly less neu expression than those that emerged in the neu-tg (Fig. 2, *B* and *C*). Cell lines established from the ANVs maintained low Ag expression in vitro in all cases, an example (i.e., ANV1) of which is shown in Fig. 2*D*. The loss or reduction in neu expression was due, at least in part, to reductions in rat neu-specific mRNA (Fig. 2*G*). To verify that neu was not just simply internalized, we also evaluated for expression in ANV cell lines using Western blotting. Only a very weak neu-specific signal was observed in the cell lysates from various ANVs, which is consistent with flow cytometry results (Fig. 2*H*). Quantitative analysis of the ANVs compared with the fresh tumors from the neu-tg mouse, as assessed by flow cytometry, is shown in Fig. 2*I*. Unlike MMC (Fig. 1*A*), these ANV rapidly gave rise to tumor in both the neu-tg and the FVB/N parental mice (Fig. 2*I*). Because the possibility existed that the ANV tumors were derived from the FVB/N parental mice and not the transplanted tumor, PCR analysis was done, which confirmed that the ANVs contained a copy of the rat neu gene demonstrating its origin in the neu-tg (data not shown). Furthermore, the observation that these cells are tumorigenic when reimplanted (Fig. 2*J*) demonstrates that the cells were not contaminating stroma. Tumors have also been reported to lose MHC class I expression, which could lead to immune escape. Therefore, we also examined for expression of MHC class I, both basal levels and following IFN treatment. ANV cells retain MHC class I expression and can be induced to express more with either IFN-γ or IFN-α. Representative histograms for MMC and ANV1 are shown in Fig. 3, *B* and *C*.

Ag loss requires $CD4^+$ T cells

To determine the T cell subset that is primarily responsible for rejection of MMC tumor, either the $CD8^+$ or $CD4^+$ T cell subsets were depleted using mAbs before tumor injections. As shown in

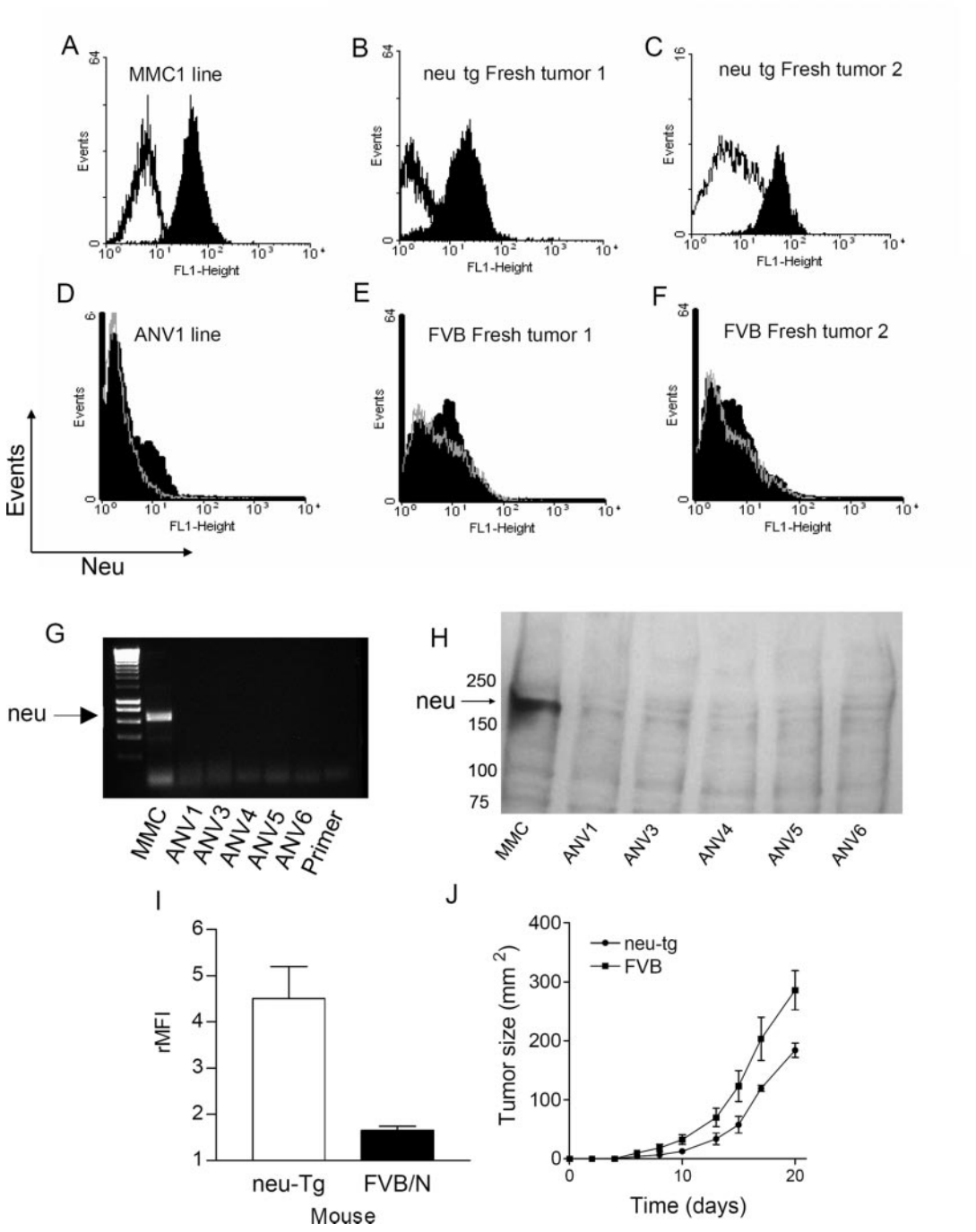

FIGURE 2. Tumors that emerge in FVB/N parental mice following MMC rejection are Ag-low variants or ANVs. *A–F*, Histograms of neu expression in either cell lines (*A* and *D*) or fresh tumors derived from neu-tg mice (*B* and *C*) and FVB/N mice (*E* and *F*). Data shown are representative of three similar and independent experiments. *A–C*, Control data are shown as open black line histogram. *D–F*, Control data are shown as gray line histogram. *G*, RT-PCR analysis of rat neu expression of MMC and several Ag-low or ANV lines (ANV1, 3, 4, 5, and 6). The DNA ladder (*far left lane*) is shown. *H*, Protein expression, as assessed by immunoblotting, of rat neu in the ANV cells lines of *G* relative to expression of expression in MMC. The arrow indicates the band corresponding to rat neu. Values (*left*) are the positions of the molecular weight markers. *I*, The average (± SEM) relative mean fluorescent intensity (rMFI) of neu staining in tumors derived from either the neu-tg or FVB/N mice. *J*, An example ANV cell line growing unimpeded in both FVB/N and neu-tg mice. Each measurement represents the mean (± SEM) of three mice. The experiment was repeated twice with similar results.

Fig. 4*A*, only those animals depleted of $CD4^+$ T cells were unable to reject the tumor cells. Tumors removed from these animals showed levels of neu expression that were comparable to the MMC tumor cells, demonstrating that T cells are required for rejection and Ag-loss (Fig. 4*B*).

ANV are derived from MMC as a result of EMT

Compared with MMC, the ANV cells were morphologically distinct, being more spindle-shaped (Fig. 5, *A* and *B*). The ANV also formed less tight junctions than did the MMC, which suggested that the cells underwent EMT. Thus, an EMT cluster was derived

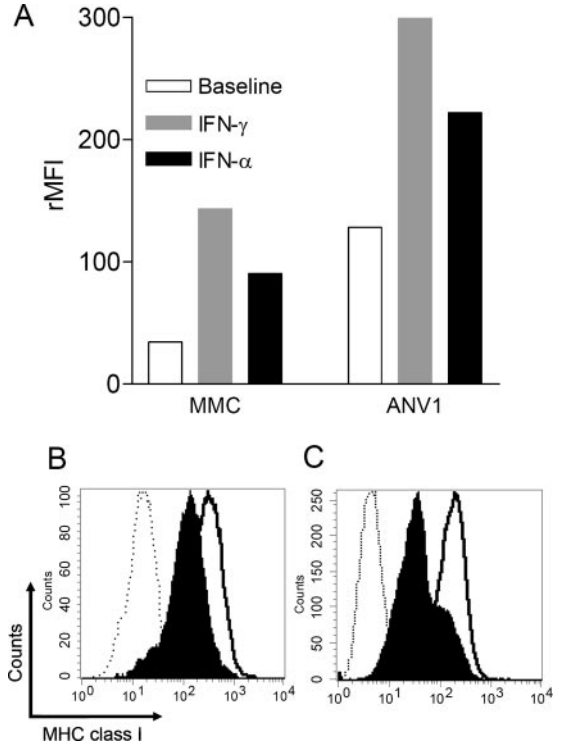

FIGURE 3. ANV cells retain MHC class I expression and responsiveness to IFN treatment. *A*, The relative mean fluorescent intensity (rMFI) of MHC class I expression on cultured MMC and ANV1 in response to IFN-γ (▨) or IFN-α as compared with baseline expression. MMC (*B*) and ANV (*C*) stained with either an irrelevant Ab (dotted histogram) or with anti-MHC class I Abs (filled and open histograms) following treatment with either medium alone (filled histogram) or IFN-γ (open histogram).

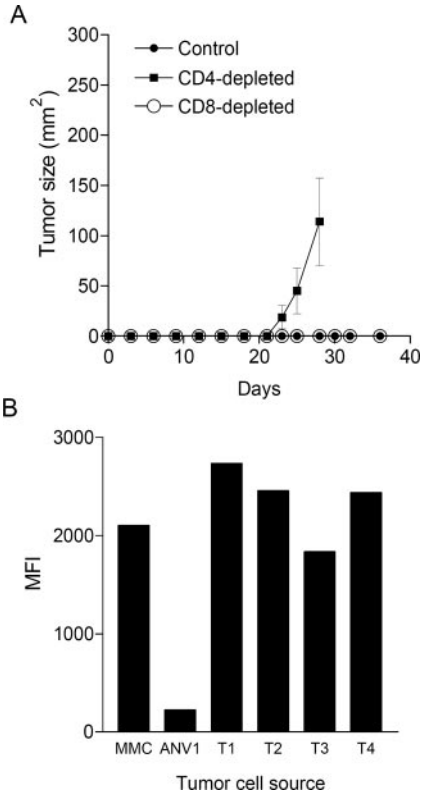

FIGURE 4. Tumor rejection and immunoediting can be eliminated by prior depletion of FVB/N mice with anti-CD4 mAbs. *A*, Tumor growth in groups of mice ($n = 4$ per group) pretreated with PBS (Control), anti-CD4 Ab, or anti-CD8 Ab. Each plot is calculated from four mice, each injected with 3×10^6 MMC tumor cells. In this experiment, the animals were not followed to relapse. The symbols for the control and the CD8-depleted T cell subsets overlap. *B*, Mean fluorescence intensity (MFI) of tumor cells (T1-T4), derived from anti-CD4 treated mice and stained with rat neu-specific Abs as compared with either MMC (neu^+) or ANV1 (neu^-).

from a RNA microarray and used to examine for evidence of EMT. The cluster consisted of E-cadherin (Fig. 5*C*) and TJP1 (ZO1) (Fig. 5*D*) for epithelial cell markers and N-cadherin (Fig. 5*E*) and vimentin (Fig. 5*F*) for mesenchymal cell markers (20–22). As shown, the pattern of gene expression demonstrates that ANVs are mesenchymal, having reduced expression of E-cadherin and TJP1 and elevated levels of N-cadherin and vimentin. PCR confirmed the results of the microarray by showing that TJP is down-regulated and vimentin is up-regulated in the ANV (Fig. 5*G*). Analysis of five other independent Ag-loss variant cell lines by RT-PCR demonstrated loss of E-cadherin confirming loss of epithelial characteristics (Fig. 5*H*). Lastly, we also examined for cell surface expression of CD24, a marker whose level of expression in the mammary gland distinguishes epithelial cells from nonepithelial cells (23). As shown in Fig. 5, *I* and *J*, the transition of MMC to ANV was accompanied by a reduction in CD24 expression.

ANV demonstrate a more invasive phenotype than MMC

EMT is a cellular reprogramming strategy that is used early in the course of embryonic development to impart a migratory and invasive phenotype to epithelial cells so that they may migrate to other regions to give shape to the developing embryo (24). Furthermore, EMT has recently been implicated as a mechanism important for local tumor invasion and metastasis (25, 26). Thus, we speculated that ANV cell lines because of EMT may express molecules associated with increased invasion. Using microarray, again we examined expression of a panel of matrix metalloproteinases (MMPs), enzymes that are involved in their increased invasive potential (27). Of the eight metalloproteinases in the cluster, the MMC expressed two predominantly, MMP2 and MMP9 (Fig. 6*A*). Consistent with a more invasive phenotype, the ANV acquired expression of MMP3, MMP10, MMP11, MMP13, and MMP14, which were not expressed at all in the MMC cells. Furthermore, the ANV also demonstrated expression, in contrast to MMC, of other tumor invasion-associated proteins such as Twist (20), Slug (20), and SDF-1 (28) (as shown in Fig. 2*B*). Both Twist and Slug are also intricately involved in the EMT process (20). The ANV cells were also more invasive as assessed by in vitro migration assays as shown in Fig. 6*C*. The expression of these increased invasion markers, however, did not appear to confer an increased growth advantage because MMC and ANV grew largely at the same rate following transplantation, indicating that EMT may result in increased invasion without altering overall growth rate (Fig. 6*D*).

Discussion

According to the premise of immunosurveillance and immunoediting, immunoescape is a multifaceted event. Tumors can either shut off the immune response (e.g., tolerance induction) or alter their phenotype to lose or avoid recognition (e.g., immunoediting). Past research demonstrating that strong immune responses can lead to the generation of Ag-loss variants has suggested that immunoediting is frequent and can lead to the generation of tumors to which the immune system is tolerant. Using the neu-tg mouse model of epithelial breast cancer, in the present study, we have investigated the phenotype of tumor cells that have undergone immunoediting.

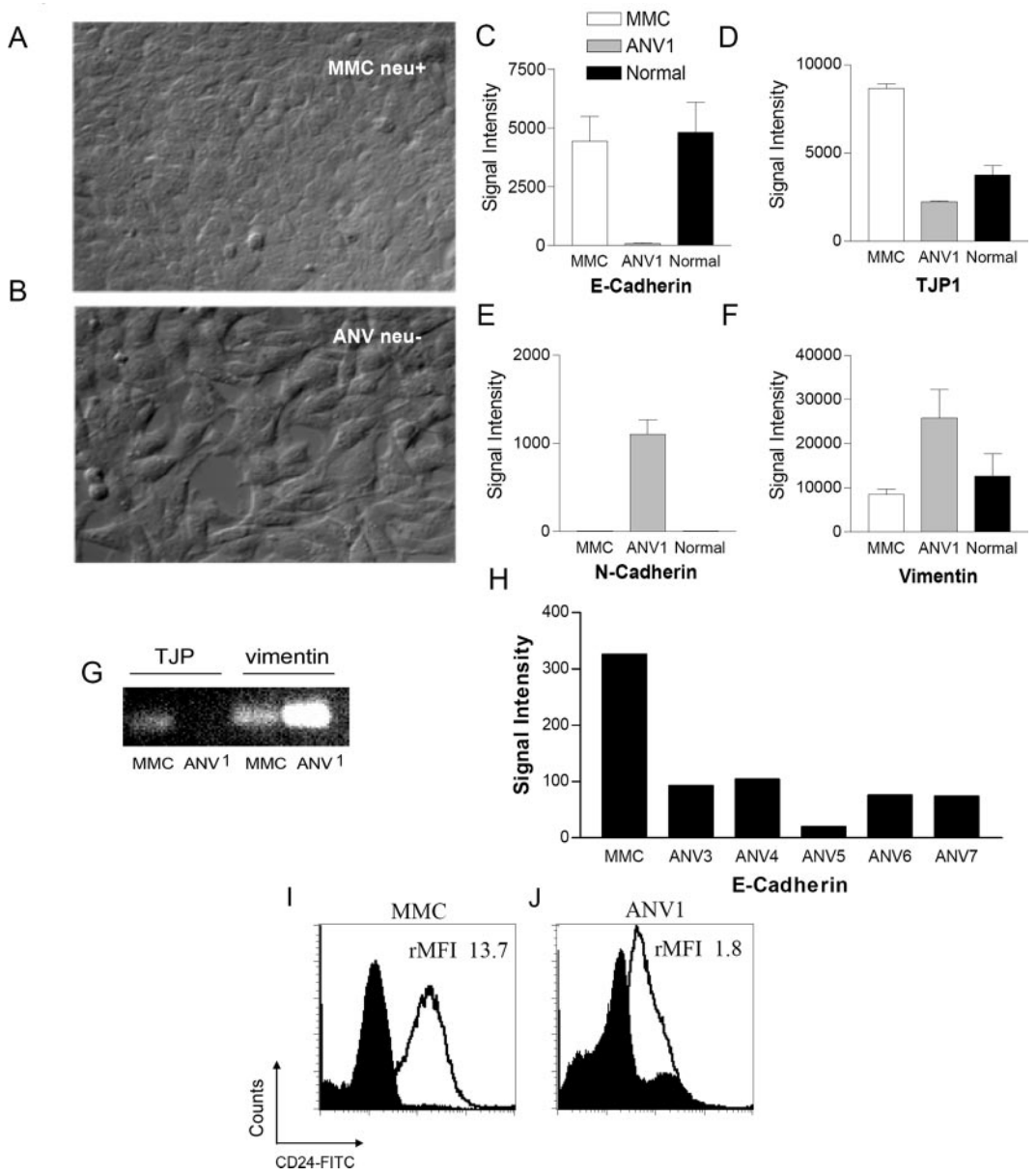

FIGURE 5. ANV are derived from MMC as a result of EMT. Microscope view of the MMC (*A*) and ANV1 (*B*) are shown. *C–F*, Microarray data for EMT markers, E-cadherin, TJP1, N-cadherin, and vimentin are shown. Data represent the mean (± SEM) of two signal intensity measurements from the Affymetrix 420 2.0 array. Similar results were repeated in similar independent experiments using two different microarray analyses. *G*, PCR confirmation of the microarray results for TJP1 and vimentin in the MMC and ANV1 cells. *H*, Quantitative PCR analysis of E-cadherin loss, compared with MMC cell line, in various tumor cell lines generated from tumors derived following immunoediting. The experiment was repeated twice with similar results. *I* and *J*, Histograms of MMC and ANV1 cells stained for CD24 expression are shown. Value shown (*inset*) is the relative mean fluorescence intensity (rMFI) for each cell line.

Specifically, we have found that the tumor cells lost Ag expression, had an altered morphology, and up-regulated genes associated with EMT.

In recent years, the concept of immunoediting has become important because the generation of ANVs in vivo with immune-based approaches is being reported more frequently by a number of laboratories not only in breast cancer but also other cancers following immune-based therapies using a number of different strategies. For example, we have previously reported that mAb therapy can lead to the rapid emergence of tumor ANVs in the neu-tg mouse (2). The phenotype of the resulting Ag-negative tumors was a stable phenotype and not simply due to Ab-induced protein degradation. Furthermore, we also observed in a prior study, that Ag-loss variants generated in FVB/N mice had a unique proteomic profile compared with the tumors generated in the neu-tg mouse model, which was associated with reduced immune danger signals (11). Similarly, Zhou et al. (5) recently reported that mouse renal adenocarcinoma cells can undergo Ag-loss in response to Ag-specific CD4 Th cell therapy. In that study, they observed that the model Ag of influenza hemagglutinin is lost due to down-modulation of the influenza hemagglutinin mRNA, suggesting immunoediting works at the nucleotide level. Our finding that endogenous $CD4^+$ T cells are important in immunoediting corroborates the importance of $CD4^+$ T cells in immunoediting. In humans, adoptive T cell therapy and cancer vaccines have demonstrated the potential for Ag-loss variants to emerge (3, 6, 29). For example, Dudley et al. (29) showed in clinical trials of adoptive T cell therapy with expanded melanoma-derived

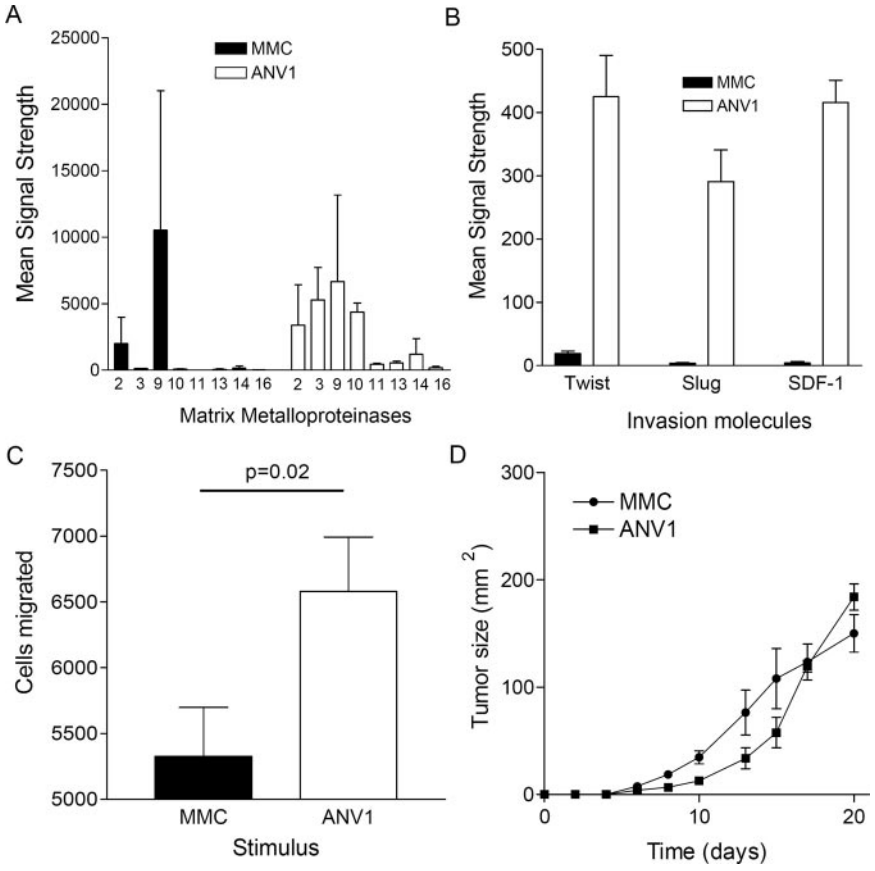

FIGURE 6. ANV tumor cells display a more invasive phenotype than MMC tumor cells. *A*, Levels of MMPs in both the MMC (■) and the ANV (□). Data are the mean (± SEM) of two integrated measurements from two independent gene chip experiments. The results for MMP2 were confirmed using dual-staining microarray. *B*, Increased expression of three proteins involved in breast cancer invasion potential. The results for stromal cell derived factor-1 were confirmed using dual-staining microarray. *C*, Invasive potential of MMC (■) and ANV (□) is represented measured as the relative mean fluorescence intensity (rMFI). Data represent the mean of six determinations. *D*, The comparative tumor development and growth of 3×10^6 MMC or ANV in neu-tg mice. Each time point is the mean (± SEM) of triplicate determinations.

tumor-infiltrating lymphocytes that responding patients, but not nonresponding patients, developed both Ag- and MHC-loss variants following treatment, demonstrating that immunoediting is important in human tumors as well. Although the mechanisms by which Ag expression is lost is not clear (i.e., genetic or epigenetic), mouse studies have begun to answer some questions. Sanchez-Perez et al. (4) have shown in the B16 melanoma model that, rather than selecting for mutants, gene expression is lost epigenetically through DNA methylation following immunoediting. Collectively, the observations that the altered phenotypes are stable and that gene expression is modulated, suggest that immunity activates cellular reprogramming pathways.

Our study suggests that one potential reprogramming mechanism activated during immunoediting is EMT, a gene expression program that has long been known to be important in embryonic development but only suspected recently to have a role in the pathogenesis of cancer (26). Embryonic epithelial tissue cells use EMT to dedifferentiate and transition into a more motile cell type to give rise to specialized tissues including the mammary glands, somites, and heart endocardium (26). Although it is unclear what role EMT plays in cellular motility in a fully developed healthy mammal, EMT is a reprogramming strategy that is used pathologically in breast cancer, which may permit nonmigratory epithelial cancer cells to acquire motility to seed other tissues within the body (30). Similar to that observed in embryonic development, the transition of breast epithelial cells to the mesenchymal state is also accompanied by a loss of epithelial characteristics (e.g., E-cadherin, TJPs) as well as tissue-specific proteins (our unpublished observations). Thus, these results suggest that the interaction of tumor cells with the immune system may not only result in loss of immune recognition but also may have a role in the pathogenesis of the disease.

With the exception that $CD4^+$ T cells are required, at present we can only speculate on the potential in vivo mechanisms by which the immune system could lead to EMT. In a recent report, Bates and Mercurio (31) demonstrated a connection between the immune system and the induction of EMT by showing that activated macrophages could directly facilitate EMT in human colonic tumor cells in vitro. Further analysis revealed that TNF-α was a critical factor produced by the macrophages that led to accelerated EMT. Thus, a plausible scenario that may explain our findings is that the immune effectors (T cell, macrophages, etc) at the tumor site led to increased levels of TNF-α. Indeed, this result may have a correlate in human breast cancer where increased TNF-α in the tumor microenvironment in the periphery is associated with increased metastatic potential (32, 33). Alternatively, other immune factors are also associated with EMT. For example, EMT is typically induced by TGF-β in a variety of different cell types including breast cancer cells in vitro (34). Furthermore, several immune effectors such as regulatory T cells are known to produce high levels of TGF-β (35). Thus, the development of a strong immune response may also be accompanied by chemoattraction or induction of TGF-β producing regulatory T cells that may also promote EMT. Nonetheless, understanding the mechanisms of EMT induction in the immune microenvironment will improve our understanding of tumor-immune interactions and the development of immune escape variants.

In conclusion, our findings suggest that immunoediting of breast tumors in mice may involve EMT. Thus, immune escape may be more than incremental changes in gene expression resulting in the chance loss of Ag expression. Rather, breast cancer may actively escape immune detection through the pathologic use of cellular reprogramming.

Acknowledgments

The expert technical assistance of Shay Park and Dr. Christopher Krco is gratefully acknowledged. We gratefully acknowledge helpful discussions from Dr. Masoud Manjili.

Disclosures

The authors have no financial conflict of interest.

References

1. Dunn, G. P., A. T. Bruce, H. Ikeda, L. J. Old, and R. D. Schreiber. 2002. Cancer immunoediting: from immunosurveillance to tumor escape. *Nat. Immunol.* 3: 991–998.
2. Knutson, K. L., B. Almand, Y. Dang, and M. L. Disis. 2004. Neu antigen-negative variants can be generated after neu-specific antibody therapy in neu transgenic mice. *Cancer Res.* 64: 1146–1151.
3. Yee, C., J. A. Thompson, D. Byrd, S. R. Riddell, P. Roche, E. Celis, and P. D. Greenberg. 2002. Adoptive T cell therapy using antigen-specific $CD8^+$ T cell clones for the treatment of patients with metastatic melanoma: in vivo persistence, migration, and antitumor effect of transferred T cells. *Proc. Natl. Acad. Sci. USA* 99: 16168–16173.
4. Sanchez-Perez, L., T. Kottke, R. M. Diaz, A. Ahmed, J. Thompson, H. Chong, A. Melcher, S. Holmen, G. Daniels, and R. G. Vile. 2005. Potent selection of antigen loss variants of B16 melanoma following inflammatory killing of melanocytes in vivo. *Cancer Res.* 65: 2009–2017.
5. Zhou, G., Z. Lu, J. D. McCadden, H. I. Levitsky, and A. L. Marson. 2004. Reciprocal changes in tumor antigenicity and antigen-specific T cell function during tumor progression. *J. Exp. Med.* 200: 1581–1592.
6. Khong, H. T., Q. J. Wang, and S. A. Rosenberg. 2004. Identification of multiple antigens recognized by tumor-infiltrating lymphocytes from a single patient: tumor escape by antigen loss and loss of MHC expression. *J. Immunother.* 27: 184–190.
7. Lozupone, F., L. Rivoltini, F. Luciani, M. Venditti, L. Lugini, A. Cova, P. Squarcina, G. Parmiani, F. Belardelli, and S. Fais. 2003. Adoptive transfer of an anti-MART-$1_{27–35}$-specific $CD8^+$ T cell clone leads to immunoselection of human melanoma antigen-loss variants in SCID mice. *Eur. J. Immunol.* 33: 556–566.
8. Madjd, Z., I. Spendlove, S. E. Pinder, I. O. Ellis, and L. G. Durrant. 2005. Total loss of MHC class I is an independent indicator of good prognosis in breast cancer. *Int. J. Cancer* 117: 248–255.
9. Bissell, M. J., and M. A. Labarge. 2005. Context, tissue plasticity, and cancer: are tumor stem cells also regulated by the microenvironment? *Cancer Cell* 7: 17–23.
10. Ercolini, A. M., B. H. Ladle, E. A. Manning, L. W. Pfannenstiel, T. D. Armstrong, J.-P. Machiels, J. G. Bieler, L. A. Emens, R. T. Reilly, and E. M. Jaffee. 2005. Recruitment of latent pools of high-avidity $CD8^+$ T cells to the antitumor immune response. *J. Exp. Med.* 201: 1591–1602.
11. Manjili, M. H., H. Arnouk, K. L. Knutson, M. Kmieciak, M. L. Disis, J. R. Subjeck, and A. L. Kazim. 2006. Emergence of immune escape variant of mammary tumors that has distinct proteomic profile and a reduced ability to induce "danger signals". *Breast Cancer Res. Treat.* 96: 233–241.
12. Guy, C. T., M. A. Webster, M. Schaller, T. J. Parsons, R. D. Cardiff, and W. J. Muller. 1992. Expression of the neu protooncogene in the mammary epithelium of transgenic mice induces metastatic disease. *Proc. Natl. Acad. Sci. USA* 89: 10578–10582.
13. Ercolini, A. M., J.-P. Machiels, Y. C. Chen, J. E. Slansky, M. Giedlen, R. T. Reilly, and E. M. Jaffee. 2003. Identification and characterization of the immunodominant rat HER-2/neu MHC class I epitope presented by spontaneous mammary tumors from HER-2/neu-transgenic mice. *J. Immunol.* 170: 4273–4280.
14. Reilly, R. T., J.-P. Machiels, L. A. Emens, A. M. Ercolini, F. I. Okoye, R. Y. Lei, D. Weintraub, and E. M. Jaffee. 2001. The collaboration of both humoral and cellular HER-2/neu-targeted immune responses is required for the complete eradication of HER-2/*neu*-expressing tumors. *Cancer Res.* 61: 880–883.
15. Reilly, R. T., M. B. Gottlieb, A. M. Ercolini, J.-P. Machiels, C. E. Kane, F. I. Okoye, W. J. Muller, K. H. Dixon, and E. M. Jaffee. 2000. HER-2/*neu* is a tumor rejection target in tolerized HER-2/*neu* transgenic mice. *Cancer Res.* 60: 3569–3576.
16. Knutson, K. L., and M. L. Disis. 2001. Expansion of HER2/neu-specific T cells ex vivo following immunization with a HER2/neu peptide-based vaccine. *Clin. Breast Cancer* 2: 73–79.
17. Knutson, K. L., Y. Dang, H. Lu, J. Lukas, B. Almand, E. Gad, E. Azeke, and M. L. Disis. 2006. IL-2 immunotoxin therapy modulates tumor-associated regulatory T cells and leads to lasting immune-mediated rejection of breast cancers in neu-transgenic mice. *J. Immunol. In press.*
18. Drebin, J. A., V. C. Link, and M. I. Greene. 1988. Monoclonal antibodies reactive with distinct domains of the neu oncogene-encoded p185 molecule exert synergistic anti-tumor effects in vivo. *Oncogene* 2: 273–277.
19. Knutson, K. L., and M. L. Disis. 2004. IL-12 enhances the generation of tumour antigen-specific Th1 CD4 T cells during ex vivo expansion. *Clin. Exp. Immunol.* 135: 322–329.
20. Huber, M. A., N. Kraut, and H. Beug. 2005. Molecular requirements for epithelial-mesenchymal transition during tumor progression. *Curr. Opin. Cell Biol.* 17: 548–558.
21. Larue, L., and A. Bellacosa. 2005. Epithelial-mesenchymal transition in development and cancer: role of phosphatidylinositol 3′ kinase/AKT pathways. *Oncogene* 24: 7443–7454.
22. Thomson, S., E. Buck, F. Petti, G. Griffin, E. Brown, N. Ramnarine, K. K. Iwata, N. Gibson, and J. D. Haley. 2005. Epithelial to mesenchymal transition is a determinant of sensitivity of non-small-cell lung carcinoma cell lines and xenografts to epidermal growth factor receptor inhibition. *Cancer Res.* 65: 9455–9462.
23. Sleeman, K. E., H. Kendrick, A. Ashworth, C. M. Isacke, and M. J. Smalley. 2006. CD24 staining of mouse mammary gland cells defines luminal epithelial, myoepithelial/basal and non-epithelial cells. *Breast Cancer Res.* 8: R7.
24. Hay, E. D. 1995. An overview of epithelio-mesenchymal transformation. *Acta Anat. (Basel)* 154: 8–20.
25. Gotzmann, J., M. Mikula, A. Eger, R. Schulte-Hermann, R. Foisner, H. Beug, and W. Mikulits. 2004. Molecular aspects of epithelial cell plasticity: implications for local tumor invasion and metastasis. *Mutat. Res.* 566: 9–20.
26. Thiery, J. P. 2003. Epithelial-mesenchymal transitions in development and pathologies. *Curr. Opin. Cell Biol.* 15: 740–746.
27. Vihinen, P., R. Ala-aho, and V. M. Kahari. 2005. Matrix metalloproteinases as therapeutic targets in cancer. *Curr. Cancer Drug Targets* 5: 203–220.
28. Kang, H., G. Watkins, C. Parr, A. Douglas-Jones, R. E. Mansel, and W. G. Jiang. 2005. Stromal cell derived factor-1: its influence on invasiveness and migration of breast cancer cells in vitro, and its association with prognosis and survival in human breast cancer. *Breast Cancer Res.* 7: R402–R410.
29. Dudley, M. E., J. R. Wunderlich, J. C. Yang, R. M. Sherry, S. L. Topalian, N. P. Restifo, R. E. Royal, U. Kammula, D. E. White, S. A. Mavroukakis, et al. 2005. Adoptive cell transfer therapy following non-myeloablative but lymphodepleting chemotherapy for the treatment of patients with refractory metastatic melanoma. *J. Clin. Oncol.* 23: 2346–2357.
30. Vincent-Salomon, A., and J. P. Thiery. 2003. Host microenvironment in breast cancer development: epithelial-mesenchymal transition in breast cancer development. *Breast Cancer Res.* 5: 101–106.
31. Bates, R. C., and A. M. Mercurio. 2003. Tumor necrosis factor-α stimulates the epithelial-to-mesenchymal transition of human colonic organoids. *Mol. Biol. Cell* 14: 1790–1800.
32. Ardizzoia, A., P. Lissoni, F. Brivio, E. Tisi, M. S. Perego, M. G. Grassi, S. Pittalis, S. Crispino, S. Barni, and G. Tancini. 1992. Tumor necrosis factor in solid tumors: increased blood levels in the metastatic disease. *J. Biol. Regul. Homeostatic Agents* 6: 103–107.
33. Leek, R. D., R. Landers, S. B. Fox, F. Ng, A. L. Harris, and C. E. Lewis. 1998. Association of tumour necrosis factor α and its receptors with thymidine phosphorylase expression in invasive breast carcinoma. *Br. J. Cancer* 77: 2246–2251.
34. Huber, M. A., N. Azoitei, B. Baumann, S. Grünert, A. Sommer, H. Pehamberger, N. Kraut, H. Beug, and T. Wirth. 2004. NF-κB is essential for epithelial-mesenchymal transition and metastasis in a model of breast cancer progression. *J. Clin. Invest.* 114: 569–581.
35. Buckner, J. H., and S. F. Ziegler. 2004. Regulating the immune system: the induction of regulatory T cells in the periphery. *Arthritis Res. Ther.* 6: 215–222.